



## Ethyl Acetate Fraction in *Hedyotis Diffusa* Willd Inhibits T Cell Proliferation to Improve the Pathogenesis of Systemic Lupus Erythematosus

Yahui Lai<sup>a</sup>, JinJun Ji<sup>a</sup>, Ying Li<sup>a</sup>, Jingqun Liu<sup>a</sup>, Xinhui Lan<sup>b</sup>, Weihong Ge<sup>c</sup>, Li Xu<sup>a</sup>, Yongsheng Fan<sup>d</sup>, Bin Ding<sup>e,\*</sup>

<sup>a</sup> College of Basic Medicine, Zhejiang Chinese Medical University, Hangzhou 310053, Zhejiang, China

<sup>b</sup> The Pennsylvania State University, Pennsylvania 19019, United States of America

<sup>c</sup> College of Pharmaceutical Science, Zhejiang Chinese Medical University, Hangzhou 310053, Zhejiang, China

<sup>d</sup> First Clinical Medical College, Zhejiang Chinese Medical University, Hangzhou 310053, Zhejiang, China

<sup>e</sup> College of Life Science, Zhejiang Chinese Medical University, Hangzhou 310053, Zhejiang, China

### ARTICLE INFO

#### Keywords:

Cell proliferation  
Ethyl Acetate Fraction  
*Hedyotis Diffusa* Willd  
Network pharmacology  
STAT3  
Systemic lupus erythematosus  
T lymphocytes

### ABSTRACT

**Background:** Abnormal proliferation of T cells plays an essential role in the pathogenesis of Systemic lupus erythematosus (SLE). The pharmaceutical effect of *Hedyotis Diffusa* Willd (HDW) on SLE has been investigated previously. Nevertheless, the biomedical mechanism is still left unclear.

**Objective:** This study has been arranged to evaluate the therapeutic effect of the ethyl acetate fraction of HDW (EAHDW) on lupus mice and explore the potential therapeutic mechanism.

**Methods:** EAHDW was prepared with 80% ethanol reflex extraction followed by successive extraction, and analyzed with HPLC and UPLC-Q/TOP-MS. The potential targets and STAT3 affinity regulators were predicted with network pharmacology. The pharmaceutical effect of EAHDW was studied with MRL/lpr mice. Cytokines and autoantibodies were quantified with ELISA assays. The pathological damage of glomerulus and STAT3 expression in the kidney was detected with histochemical and immunohistochemical techniques. The cell cycle properties in cell proliferation were identified with the flow cytometry. The western blot and dual-Luciferase reporter assay were applied to evaluate translational and transcriptional activity of STAT3, respectively.

**Results:** In this study, the extraction ratio of EAHDW was 2.7±1%, in which 19 ingredients were identified. Network pharmacological analysis showed that the target genes of EAHDW were highly focused on influencing the abnormal T cell proliferation in SLE. EAHDW showed the beneficial effects on pathological changes and STAT3 expression in the glomerulus of lupus mice, and the levels of cytokines and autoantibodies in serum. In cytological study, EAHDW treatment attenuated the transcription and phosphorylation of STAT3, which inhibited T cell proliferation by prolonged S-phase of the cell cycle. A total of 5 compounds in EAHDW exhibited high docking affinity to the DNA-binding site of STAT3.

**Conclusion:** EAHDW could reduce the inflammatory response and inhibit the proliferation of T cells by interfering with the STAT3 signaling pathway, thereby playing a therapeutic effect on SLE.

### 1. Introduction

SLE is an autoimmune disease, which is more prevalent in women of fertile age (La Paglia et al., 2017). It is a chronic, recurrent, and relapsing-remitting disease, and many organs, including skin, kidneys and articulation, are involved (Durcan et al., 2019). However, the pathogenesis of the disease is still remained unknown. A recent study showed that the dysfunction of the immune system is one of the important mechanisms of the pathogenesis in the development of SLE, of which the autoimmune response is mediated by activation of autoreactive T and B lymphocytes (Caielli et al., 2019). The abnormal proliferation and activation of T cells provide enormous help to B cells synthesizing autoantibodies and release massive inflammatory cytokines that infiltrate target organs and promotes the pathogenesis of SLE (Edwards et al., 2015; Mak and Kow, 2014; Katsuyama et al., 2019). Therefore, elucidation of the T cells mediated SLE pathogenesis is benefit to improving the earlier diagnosis and treatment of SLE.

Immune cell signaling molecules is critical in SLE, such as signal transducer and activator of transcription-3 (STAT3), which can be activated by protein tyrosine phosphatases (Zhang and Wei, 2020). Numerous studies have demonstrated that STAT3 participates in regulating T

cells provide enormous help to B cells synthesizing autoantibodies and release massive inflammatory cytokines that infiltrate target organs and promotes the pathogenesis of SLE (Edwards et al., 2015; Mak and Kow, 2014; Katsuyama et al., 2019). Therefore, elucidation of the T cells mediated SLE pathogenesis is benefit to improving the earlier diagnosis and treatment of SLE.

Immune cell signaling molecules is critical in SLE, such as signal transducer and activator of transcription-3 (STAT3), which can be activated by protein tyrosine phosphatases (Zhang and Wei, 2020). Numerous studies have demonstrated that STAT3 participates in regulating T

\* Corresponding author : Bin Ding, E-mail address: [db@zcmu.edu.cn](mailto:db@zcmu.edu.cn) (B. Ding).

cell proliferation (Yang et al., 2019). STAT3 silencing T cells can prevent autoantibodies production of B cells, inflammatory cell infiltration, and the development of lupus nephritis (Durant et al., 2010; Yoshida et al., 2019; Yang et al., 2019). The phosphorylated STAT3 dimers can translocate into the nucleus to regulate the transcription of the target genes (Lin and Leonard, 2018). It has been reported that the cytokines and/or chemokines, such as IL-6, IL-10, IL-12, TNF, MCP-1, bind to the respective receptors of T cell, stimulate the phosphorylation of STAT3 (Durant et al., 2010). This phosphorylated STAT3 can promote the proliferation, differentiation and migration of T cells, and also serve as a feed back to promote the secretion of inflammatory cytokines, thereby aggravating the production of SLE disease (Durant et al., 2010; Du et al., 2019). Therefore, inhibiting the phosphorylation of STAT3 in T cells may be an effective way to melioration SLE.

The HDW is applied as a traditional Chinese medicine for thousands of years (Wang et al., 2017). It has been investigated that different preparation of (such as chloroform, ethanol extracts) HDW showed significant anti-inflammation and anti-tumor effects (Yan et al., 2017; Lin et al., 2012; Chen et al., 2016). Moreover, the anti-inflammatory ingredients maybe in the ethyl acetate fraction of HDW (Xu et al., 2018). Lin J et al. found that HDW extract can inhibit cell proliferation through IL-6 induced STAT3 pathway (Lin et al., 2015). In our group, Prof. Fan has used HDW as a major component of TCM formulas applying for SLE treatment (Chen et al., 2005), which present efficient benefits. However, less modern scientific mechanisms have been elucidated. We hypothesized that the ingredients in EAHDW can inhibit the phosphorylation of STAT3 to attenuating the proliferation and activation of T cells in SLE.

## 2. Material and Methods

### 2.1. Materials

Herbal medicine, HDW, was purchased from Changshan Tiandao (Hangzhou, China), which was identified by Prof. Yongsheng Fan, Zhejiang Chinese Medical University. Jurkat cells, 293T cells were purchased from Shanghai Cell Bank of Chinese Academy of Sciences. MTT assay kit (C0009S) and Cell cycle kit (C1052) were obtained from Biyun-tian (Shanghai, China). Cell Trace™ Cell proliferation kit (C34554) was purchased from Life Technologies (CA, USA). ELISA assay kits including TNF, IL-10, IL-12p40, IL-6, IFN, MCP-1 were purchased from Neobioscience (Shenzhen, China). A dual-luciferase reporter gene analysis kit (E1910) was purchased from Promega (Madison, USA). BCA assay kit was purchased from Yuanye (Shanghai, China). STAT3 (C-20) (sc482) and p-STAT3 (Y705) (sc7993) were purchased from Santa Cruz Biotechnology (Texas, USA). The secondary antibodies, Goat anti-Rabbit IRDYE @ 800 CW (926-32211) and Goat anti-Mouse IRDYE @ 680 (926-68070), were all from LICOR (Nebraska, USA). DMSO and other biochemical materials were obtained from Sigma-Aldrich (Missouri, USA).

### 2.2. Preparation of HDW ethyl acetate fraction

HDW (300 g) was reflux extracted twice with 80% ethanol (3 L) for 1.5 hours each time. The extracted resultants were pooled and concentrated with a rotary evaporator (RE3002, LICHEN, Shanghai). The compounds in this extract were successively partitioned with equal volume petroleum (3 ×), and ethyl acetate (5 ×). The obtained ethyl acetate extract was evaporated dried, and stored in a desiccator.

### 2.3. High-performance liquid chromatography (HPLC) analysis of EAHDW

EAHDW methanolic solution (10 μL 100 mg/mL) was loaded into an Acclaim Carbonyl C18 column (4.6 × 250 mm, 5 μm) (Thermo Fisher, USA) by a HPLC system (Thermo Fisher, Waltham, USA). And the column was eluted with increasing concentration acetonitrile (mobile phase A) in 0.1 % aqueous phosphoric acid (mobile phase B) over time (0–5 min, 10% A; 5–20 min, 20% A; 20–45 min, 40% A; 45–50

min, 58% A; 50–60 min, 71% A) with a flow rate of 0.8 mL/min. The eluting process was monitored with a diode array ultraviolet/visible (UV–VIS) detector at 254 nm. This study used 10 μL 20 mg/mL geniposide methanolic solution as the standard ingredient.

### 2.4. Characterization of the EAHDW chemical consist by UPLC-Q/TOF-MS

EAHDW methanolic solution (4 μL 1 mg/mL) was loaded into an ACQUITY UPLC BEH C18 (150 × 2.1 mm, 1.7 μm) column with a UPLC (Waters, Milford, MA, America) system. The mobile phase was a solution A (acetonitrile containing 0.1% formic acid) mixed in solution B (0.1% formic acid in water) with a specific concentration gradient over time; 0–5 min 15%–20% A; 5–32 min 20–40% A; 32–37 min 40–95% A. The flow rate is 0.3 mL/min. A TOF-MS (AB Sciex Pte. Ltd., MA, USA) model was performed on mass spectrometry with an electrospray ionization source (positive modes). The detection condition was: ion source gas 1 (Gas1): 55 psi, ion source gas 2 (Gas2): 55 psi, curtain gas (Cur): 35 psi, ion source temperature (TEM): 600°C, the electrospray voltage (ISVF): 4500/5500 eV; the mass spectrum scan range m/z: 50~1500 Da, MS scan accumulation time 0.25 s/spectrum, ion accumulation time 0.05 s/spectrum. The IDA-MS/MS with a high sensitivity mode condition was; positive and negative ion mode 60 v. The obtained molecular mass, and the secondary spectrum data, were comparatively screened with SCIEXOS, an ingredients database including more than 1500 Chinese herbal medicines. And the identity components were used for the following analysis.

### 2.5. Network pharmacology analysis

The potential targets of EAHDW ingredients were obtained by screening the followed four databases; traditional Chinese medicine system pharmacology technology platform (TCMSP), Pharm Mapper server based on reverse pharmacophore matching, SEA Online Search Tools and STITCH 4.0. Cytoscape 3.2.1 software was engaged to create a network of active ingredients-target genes. Simultaneously, the collected targets of lupus nephritis were constructed to form a compound-target-disease network for topological analysis and core target screening. Finally, KEGG enrichment analysis was engaged in the signaling-pathway annotation of the core target.

### 2.6. Animals grouping and treatment

MRL/lpr lupus mice, a total of 18, SPF grade, 6–8 weeks old, female, 22±2g, were purchased from the Laboratory Animal Center of Zhejiang Chinese Medical University. The mice were handled under SPF condition; 40% to 60% relative humidity, 20°C room temperature, light for 12 hours/day, free for water and food. The animals' growth and treatment followed the laboratory's principles of national standards GB14925-2001 (Laboratory Animal-Requirement of Environment and Housing Facilities). These MRL/lpr lupus mice were randomly divided into 3 groups: model group (M), EAHDW low-dose group (EAHDW-L group), and EAHDW high-dose group (EAHDW-H group). The mice in EAHDW-L and EAHDW-H groups were intragastrically administrated 100 and 200 mg/kg body weight EAHDW (suspended in sodium carboxymethyl cellulose water solution) every day. Moreover, the mice in the M group were administrated the same volume sodium carboxymethyl cellulose water solution. The mice were fed in 60 days.

### 2.7. Immunohistochemistry–image and H&E staining

The formalin-fixed and paraffin-embedded mice kidney tissue were cut into thin sections (4.5 μm) and sealed with 3% H<sub>2</sub>O<sub>2</sub> at room temperature for 30 min. Then, the sections were boiled in 10 mM sodium citrate buffer (pH 6.0) for 10 min and cooled at room temperature. For immunohistochemistry analysis, the sections were blocked with normal goat serum and then hybridized with primary antibodies against

STAT3 overnight at 4°C. The primary antibodies were detected with HRP-labeled secondary antibodies. Simultaneously, hematoxylin and eosin (H&E) staining was performed to stain the sections.

## 2.8. ELISA Assay to evaluate the concentration of cytokines and autoantibodies in sera

Concentrations of tumor necrosis factor (TNF), interleukin-10 (IL-10), interleukin-6 (IL-6), Interferon (IFN), interleukin-12 (IL-12), macrophage chemoattractant protein-1 (MCP-1), and the antinuclear (ANA), anti-double stranded (dsDNA), anti-SnRNP/Sm antibodies in serum were determined with the specific ELISA assay kits, following the kit's instruction. Briefly, 100 µL successively diluted standard cytokines and test samples were pipetted into 96-well plate, separately. After then, the 96-well plates were sealed and incubated for 2 h at 37°C. After then, the 96-well plate was emptied and washed 5 times with washing buffer (supplied with the kits). The biotin-labeled specific antibody was added to capture the respective cytokine. Furthermore, the contained biotin was quantified with a chromogenic reaction (supplied with the kits).

## 2.9. Cell tracking and proliferation studies

The cell tracking and proliferation studies (CFSE) probe were used to determine cell proliferation. Briefly, Jurkat cells were stained with 5 µM CFSE (Cell Trace™ Violet Cell Proliferation Kit) for 30 min at 37°C in the dark, then seeded in 6-well plates at a density of  $1.5 \times 10^6$  cells/mL in 2 mL medium according to the manufacturer's protocol. Subsequently, cells were exposed to a series of concentrations of EAHDW for 72 h. The CFSE fluorescence was detected using a Fluorescence-Activated Cell Sorting (FACS) Caliber instrument (BD Biosciences, San Jose, CA, USA).

## 2.10. Cell cycle detection

A total of  $1 \times 10^6$  Jurkat cells were seeded into six-well plates contained 2 mL medium and treated with 20, 40, 60, 80 µg/mL EAHDW for 24 h. The cells were harvested and adjusted to a concentration of  $1 \times 10^6$  cells/mL. Moreover, the cell was stained with a propidium iodide (PI) supplied with a cell cycle assay kit, and the Jurkat cells were analyzed with FACS. Detailly, the cells were fixed in 70% cold ethanol at 4°C overnight, then the fixed cells were washed twice with cold PBS and incubated for 30 min in the dark with RNase (8 µg/mL) and PI (10 µg/mL). The fluorescence signal was detected through the FL1 channel of the flow cytometer, and proportion of DNA in various phases of the cell cycle was analyzed using ModFit LT software (Verity Software House, Inc., Topsham, ME, USA).

## 2.11. Signal pathway detection by dual-luciferase reporter assay

The regulative capability of EAHDW on STAT3 and sis-inducible reaction element (SIE) were determined with a dual-luciferase reporter assay. The 293T cells were grown in 48-well plates and transfected with respective plasmids for 24 h, separately. Afterward, these transfected cells were treated with different concentrations of EAHDW (1, 6.25, 12.5, 25, 50, 75, 100 µg/mL) and Leukemia Inhibitory Factor (LIF, Millipore, MA, USA) for 24 h. The cells in each well were lysed, and the fluorescence signal was detected by Dual-Luciferase® Reporter Assay (Promega, USA).

## 2.12. Western blot

Jurkat cells were pre-treated with 10, 20, 40, 60, 80 µg/mL EAHDW for 24 h. Subsequently, LIF stimulation was performed for 30 min. These treated cells were lysed with lysis buffer containing protein inhibitors, and the total protein concentrations were determined by performing a BCA protein assay kit. The proteins of each cell lysate were separated with sodium dodecyl sulfate-polyacrylamide gel electrophoresis (SDS-PAGE) and transferred onto polyvinylidene difluoride membrane. The

membrane was blocked for 2 h with 5% non-fat milk/TBST buffer, then incubated with the primary antibody, specific against STAT3, p-STAT3 (dilution, 1:1,000), overnight at 4°C. The next day, membranes were washed and incubated with the respect secondary antibody (LICOR, Nebraska, USA) for 2 hours. The blots were exposed and scanned using an Odyssey Infrared Imaging system (LI-COR Biosciences).

## 2.13. Molecular docking

Compounds from EAHDW were included in analyzing their affinity with STAT3. The STAT3 protein molecular model (PDB ID: 3CWG) is an X-ray crystal structure of an unphosphorylated STAT3 fragment obtained from Research Collaboratory for Structural Bioinformatics Protein Data Bank (<http://www.rcsb.org/>). The 3D structure of the ingredient was obtained in the PubChem. Firstly, the crystal water in the 3D structure of STAT3 protein was replaced by polar hydrogen atoms with AutodockTools (Trott and Olson, 2010). The lower the binding force score obtained, the better the binding effect.

## 2.14. Statistical analysis

All the data in this study were expressed as mean ± standard deviation (SD). The data was analyzed using SPSS software package for Windows (version 17.0; SPSS, Inc., Chicago, IL, USA), and one-way analysis of variance was used to compare multiple groups. The statistically significance difference was considered at level  $P < 0.05$ .

## 3. Results

### 3.1. Preparation and constituents of EAHDW

EAHDW was prepared with ethanolic reflux extraction, followed by sequential extraction based on the different solubilities of the extracted components. A total of  $8.12 \pm 3.8$  g EAHDH was obtained from 300 g dried HDW. The extraction ratio was  $2.7 \pm 1\%$ . The EAHDW was comparatively analyzed with geniposide, which was shown in Figure 1A. The concentration of geniposide in EAHDW was 8.21%, which was calculated with peak area. The chemical constituents in EAHDW were analyzed with UPLC-Q/TOF-MS. Here we show the total ion current chromatogram in positive ion mode (Figure 1B). By comparing and screening with the accurate primary mass, isotope distribution ratio, and MS/MS of the compound TCM MS/MS Library in the secondary database of traditional Chinese medicine that comes with the SCIEX OS software. A total of 19 compounds were identified with the positive ion mode, which marked from 1-19 in the Figure 1 B. And the area, Retention Time, Mass Error, Library Score and Isotope Ratio Difference of the compound were listed in Table 1.

### 3.2. Network pharmacological study predicted target gene of EAHDW

Network analysis was attempted to facilitate scientific interpretation of the complicated relationships among herb ingredients, diseases, and genes. Firstly, the potential gene targets of EAHDW ingredients were explored and finally obtained 3116 targets, by screening and searching four databases, TCMSP, PharmMapper server, SEA online search tool, and STITCH database. And the compound-target network diagram was drafted with Cytoscape 3.4.1 software and showed in Figure 2 A. In a further study, the disease-related genes were collected by screening five databases, DrugBank, OMIM, GAD, TTD, GooLGeN, and 1121 SLE related genes were obtained. In the following, the PPI network of compound, target, and SLE diseases were constructed with a merge of compound-target and disease-target network diagrams by Cytoscape 3.4.1. This network has 8537 nodes and 200197 edges, which means 8537 genes and 200197 regulatory connections (Figure 2 B). Then use the plug-in CytoNCA to analyze the topological properties of each node in the interaction network by calculating six metrics 'betweenness centrality

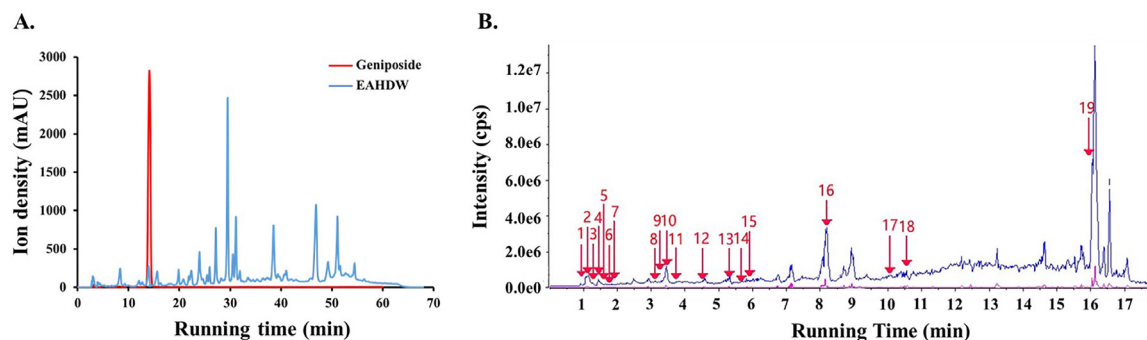


**Figure 1.** Composition analysis of EAHDW (A.) The index components in EAHDW. The HPLC chromatograms were presented the standard molecule, Geniposide (red), and EAHDW (blue) at 254 nm wavelength. (B.) UPLC-MS/MS analysis of EAHDW in positive ionization mode. The identified main appearing peaks with retention time between 1 and 12 min in total ion current (TIC) chromatogram. And the specific ingredients of EAHDW were marked from 1 to 19.

**Table 1**  
The identified compounds in EAHDW

No.	Component Name	Area	RT (min)	Formula	OB (%)	MW (g/mol)	DLindex
1	Adenine	314900	1.06	C <sub>5</sub> H <sub>5</sub> N <sub>5</sub>	62.80	135.15	0.0348
2	Betaine	166600	1.09	C <sub>5</sub> H <sub>11</sub> NO <sub>2</sub>	40.92	117.17	0.0126
3	Stachydrine	91460	1.11	C <sub>7</sub> H <sub>13</sub> NO <sub>2</sub>	0.29	144.22	0.0280
4	Vitamin B6	8995	1.12	C <sub>8</sub> H <sub>11</sub> NO <sub>3</sub>	61.54	169.2	0.0410
5	10-Deacetylasperulosidic acid	33670	1.15	C <sub>16</sub> H <sub>22</sub> O <sub>11</sub>	3.42	390.38	0.44681
6	Nicotinic acid	68920	1.43	C <sub>6</sub> H <sub>5</sub> NO <sub>2</sub>	47.64	123.12	0.0202
7	Deacetyl asperulosidic acid methyl ester	3821	1.92	C <sub>17</sub> H <sub>24</sub> O <sub>11</sub>	4.29	404.41	0.4823
8	4-Hydroxybenzoic acid	84920	3.26	C <sub>7</sub> H <sub>6</sub> O <sub>3</sub>	30.15	138.13	0.02668
9	Asperuloside	93900	3.45	C <sub>18</sub> H <sub>22</sub> O <sub>11</sub>	12.72	414.4	0.7094
10	Daphnetin	53220	3.64	C <sub>9</sub> H <sub>6</sub> O <sub>4</sub>	24.23	178.15	0.0665
11	Geniposide	7481	3.95	C <sub>17</sub> H <sub>24</sub> O <sub>10</sub>	14.64	388.41	0.4415
12	Fraxetin	63570	4.53	C <sub>10</sub> H <sub>8</sub> O <sub>5</sub>	23.04	208.18	0.0915
13	Syringaldehyde	62260	5.69	C <sub>9</sub> H <sub>10</sub> O <sub>4</sub>	67.06	182.19	0.0480
14	Isoscapoletin	1E+06	5.94	C <sub>10</sub> H <sub>8</sub> O <sub>4</sub>	23.46	192.18	0.0760
15	Isoferulic acid	66240	6.09	C <sub>10</sub> H <sub>10</sub> O <sub>4</sub>	50.83	194.2	0.0582
16	Coumarin	3E+06	8.18	C <sub>9</sub> H <sub>6</sub> O <sub>2</sub>	29.17	146.15	0.0430
17	Berberine	7181	10.16	C <sub>20</sub> H <sub>17</sub> NO <sub>4</sub>	36.86	336.39	0.7767
18	Hymecromone	371800	10.4	C <sub>10</sub> H <sub>8</sub> O <sub>3</sub>	35.09	176.18	0.0639
19	Patchouli alcohol	265700	16.12	C <sub>15</sub> H <sub>26</sub> O	101.96	222.41	0.1362

Note: RT=Retention Time, OB=Oral Bioavailability, MW=Molecular Weight, DL=Drug-Likeness

(BC), 'degree centrality (DC)', 'eigenvector centrality (EC)', 'closeness centrality (CC)', 'network centrality (NC)' and 'local average connectivity (LAC)', 736 core targets were obtained (Figure 2 B). Finally, we found that these core targets of EAHDW were highly focused on SLE (68.18%) and cell cycle (14.77%), T cell receptor, TNF and other signaling pathways, with KEGG enrichment analysis (Figure 2 C and D). In the following, we explored the therapeutic effect of EAHDW on SLE and its potential mechanism.

### 3.3. EAHDW attenuated the pathological damage of kidney in MRL/lpr

The result of the network pharmacological study indicated the SLE-influenced activity of EAHDW. Therefore, we identified this activity *in vivo* with MRL/lpr mice. The mice kidney in the model group showed inflammatory cell infiltration, mesangial hyperplasia, increased glomerular volume (Figure 3A). In comparison, these pathological changes in the mice kidneys in EAHDW-L and EAHDW-H groups were alleviated (Figure 3A). And this effect of EAHDW was dose dependent (Figure 3B).

### 3.4. EAHDW ameliorated the content of inflammatory cytokines and autoantibodies in the serum

The changes of inflammatory cytokines and autoantibodies content in the serum was a significant diagnostic analysis in SLE. Compared with the Model group, the concentration of IFN and MCP-1 ( $P < 0.05$ ),

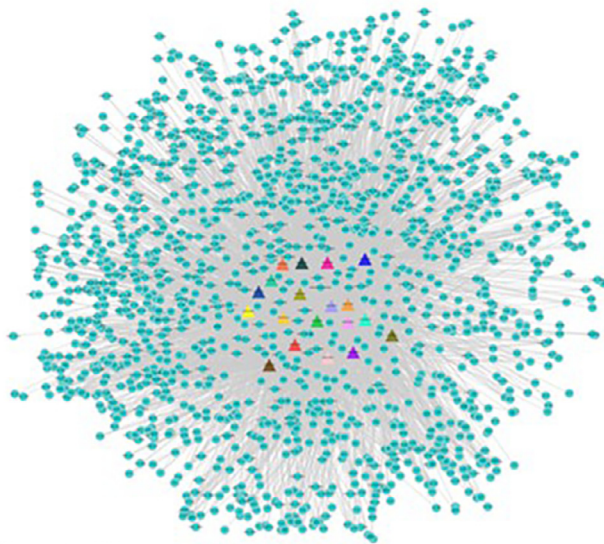
and IL-6, IL-12 ( $P < 0.005$ ) were significantly reduced by EAHDW treatment (Table 2). The concentration of ANA, Anti-dsDNA and Anti-SnRNP/Sm in the serum of EAHDW treated mice was significantly decreased ( $P < 0.05$ ) (Table 3). However, this effect of EAHDW was not dose-dependent.

### 3.5. EAHDW blocked the T cell proliferation through STAT3

The results of network pharmacology have shown that T cell cycle signaling pathways were the regulatory target of EAHDW. Jurkat cell is an immortalized T lymphocyte cell, which has been used as a prototypical T cell line in studying T cells biological events. CFSE fluorescent reagent was used to staining the Jurkat cells, which were treated with different concentration of EAHDW. The dividing Jurkat cells was decreased gradually; 78.9%, 76.1%, 69.9%, 70.7% and 62.31%, as the concentration of EAHDW increased successively; 0, 10, 20, 40 and 60  $\mu\text{g}/\text{mL}$ . (Figure 4A). Simultaneously, the percentages of cells in G2/M phases were dose-dependently gradually decreased; 25.3%, 21.6%, 8.63%, 5.63%, 0.41%, when the EAHDW concentration increased; 0, 20, 40, 60 and 80  $\mu\text{g}/\text{mL}$ , respectively. When the concentration of EAHDW increased to 40  $\mu\text{g}/\text{mL}$ , more than half of the Jurkat cells stayed at the S phase. Interestingly, 20  $\mu\text{g}/\text{mL}$  EAHDW treatment gently increased the cells' G0/G1 phase percentage (Figure 4B).

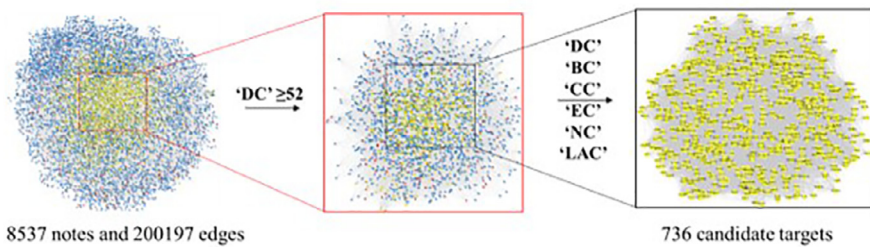
In the following, the dual-luciferase reporter gene experiment was engaged to elucidate the regulative capability of EAHDW on STAT3 in the 293T cell line. 293T cell is a renal epithelial cell line, which

A.

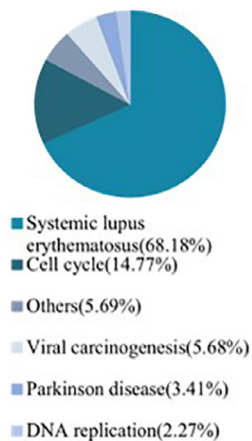


- |   |  |
|---|--|
| ▲ MOL001788 Adenine                                       | ▲ MOL004557 Geniposide +NH3              |
| ▲ MOL000430 Betaine                                       | ▲ MOL004667 Fraxetin                     |
| ▲ MOL000447 Stachydrine                                   | ▲ MOL003177 Syringaldehyde               |
| ▲ MOL011440 Vitamin B6                                    | ▲ MOL000339 Isoscooletin                 |
| ▲ MOL001664 10-Deacetylasperulosidic acid+NH3             | ▲ MOL005928 Isoferulic acid              |
| ▲ MOL000421 Nicotinic acid                                | ▲ MOL000431 Coumarin                     |
| ▲ MOL001666 Deacetyl asperulosidic acid methyl ester +NH3 | ▲ MOL001454 Berberine                    |
| ▲ MOL000103 4-Hydroxybenzoic acid                         | ▲ MOL001228 Hymecromone                  |
| ▲ MOL007785 Asperuloside                                  | ▲ MOL000695 Patchouli alcohol (loss H2O) |
| ▲ MOL005118 Daphnetin                                     | ● Target                                 |

B.



C.



D.

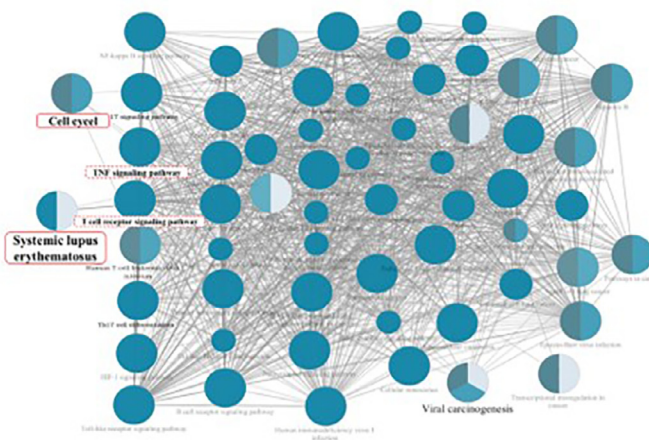


**Figure 2.** Network pharmacology analysis of EAHDW in the treatment of SLE. (A.) EAHDW compound-target network. The triangles represent the drug compound, and the dot represents the target point. (B.) Protein-protein biomolecular network diagram. From the left to right were the target of the core protein interaction (CPPI) network, the CPPI network of EAHDW (with the screening criterion Degree centrality (DC) ≥ 25), and the PPI network of the main EAHDW components (with six screening parameters DC, BC, CC, EC, NC and LAC). (C. and D.) KEGG enrichment analysis yielded the targets, which were closely related to the disease including SLE (68.18%) and cell cycle regulation (14.77%).

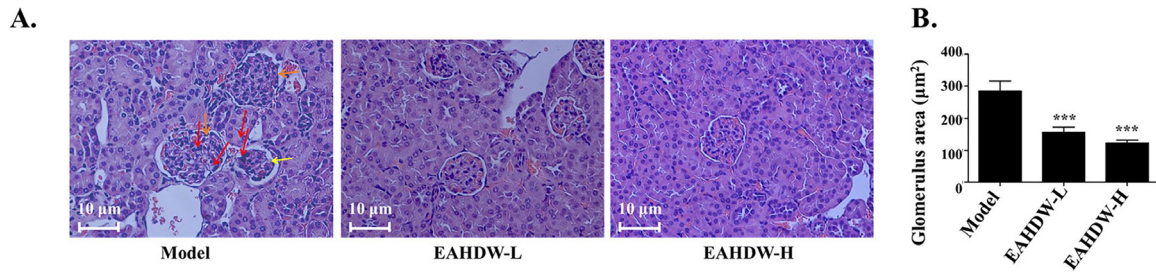


**Figure 3.** Improvement of EAHDW on kidney tissue of lupus Mice. (A) The representative images of H&E-stained kidney sections were shown (magnification 400 ×). The red arrows indicate the inflammatory cell infiltration, the yellow one indicates mesangial hyperplasia, and the orange arrows indicates the thickened basement membrane. (B) The quantitative analysis of the glomerulus area. \*\*\**P*<0.0001 vs Model.

**Table 2**  
Effect of EAHDW on Inflammatory Cytokines in lupus mice (Unit: pg/mL)

Group	IL-6	IFN	IL-12P70	TNF	MCP-1	IL-10
Model	10.24±1.17	10.29±0.65	92.62±7.30	33.60±2.84	76.18±4.38	99.07±5.51
EAHDW-L	7.32±0.90**	9.17±9.82	81.55±1.37*	28.35±1.39*	76.37±2.03	91.12±9.86
EAHDW-H	7.20±0.67**	8.23±0.52*	74.67±4.37**	29.85±0.52*	70.67±4.37*	90.01±2.26

Note: The data represent as the mean ± standard deviation of 6 mice in each group. \**P*<0.05, \*\**P*<0.005 vs Model.

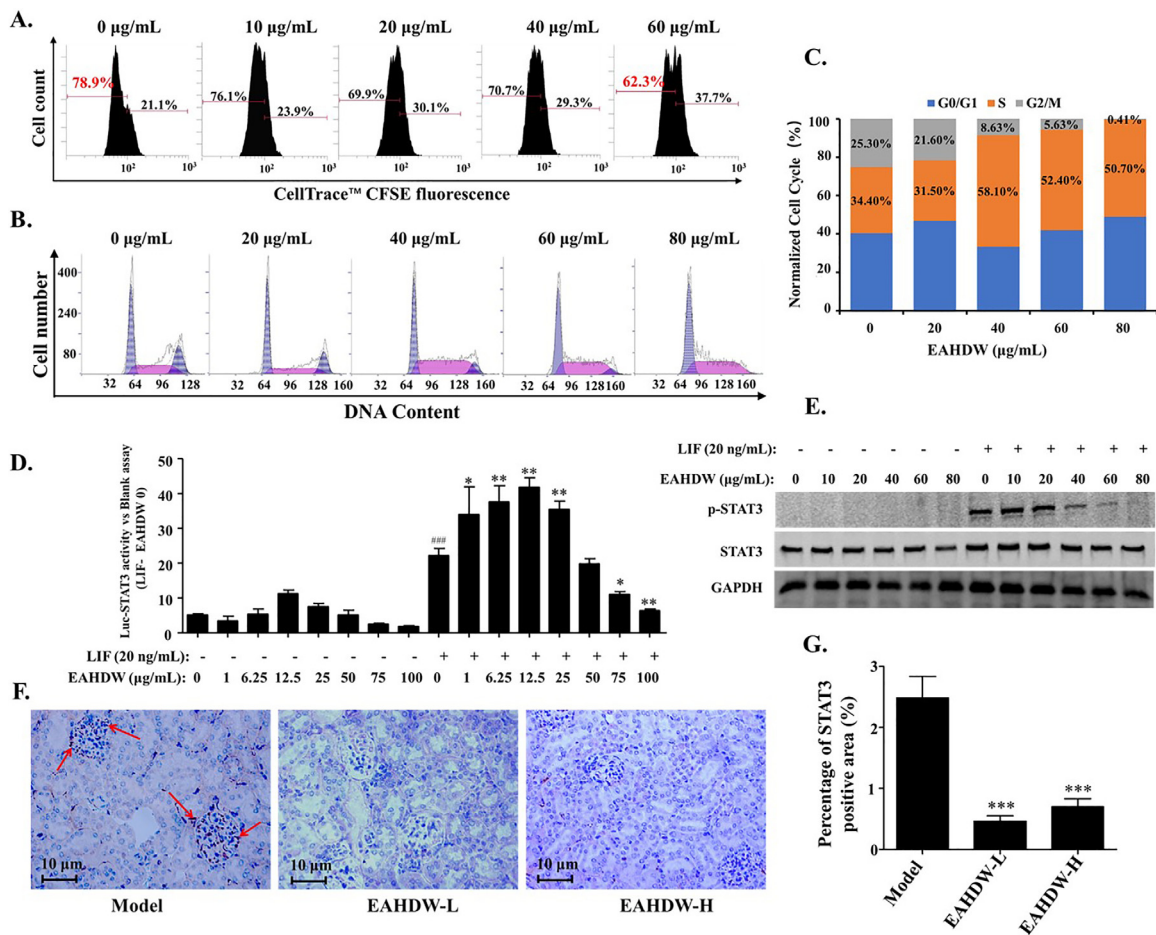


**Figure 4.** The effect of EAHDW on the proliferation and cell-cycle of T cell. (A) The effect of gradually increased EAHDW on Jurkat cells proliferation were detected by CFSE staining and flow cytometric analysis. (B) The effect of EAHDW on the cell-cycle of Jurkat cells was analyzed by flow cytometry. (C) The relative frequency of cells was shown with the bar chart. (D) The effect of EAHDW on the transcription of STAT3 were evaluated with dual-luciferase reporter assay. The data showed as the mean ± standard deviation of 3 replications. ###*P*<0.001, vs 0 µg/mL; \**P*<0.05, \*\**P*<0.01, vs LIF. (E) The effect of EAHDW on p-STAT3 protein expression in Jurkat cells. (F) The immunohistochemical study of STAT3 expression (red arrows) in kidneys of different group mice. (G) The percentage of immunohistochemical stained area was shown with bar chart. \*\*\**P*<0.0001 vs Model.

**Table 3**  
Effect of EAHDW on autoantibodies in lupus mice. (Unit: ng/L)

Group	ANA	Anti-dsDNA	Anti-SnRNP/Sm
Model	39.76±3.98	654.17±73.15	21.78±2.82
EAHDW-L	35.53±2.65	510.70±63.30*	20.20±0.64
EAHDW-H	33.91±2.57*	598.88±53.40	18.15±0.75*

Note: The data represent the mean ± standard deviation of 6 mice in each group. \* $P < 0.05$  vs Model.

is easily transfected. The expression of STAT3 in 293T cells was relatively low, which could be slightly influenced by different concentrations of EAHDW. In comparison, LIF, a most pleiotropic member of the IL-6 cytokine family, could significantly stimulate the expression of STAT3 (###  $P < 0.001$  Figure 4C). In assays with 1, 6.25, 12.5  $\mu\text{g/mL}$  EAHDW, the expression of STAT3 were statistically increased (\*  $P < 0.05$ , \*\*  $P < 0.01$  and \*\*\*  $P < 0.001$ ), but as the concentration of EAHDW further increased (from 25 to 100  $\mu\text{g/mL}$ ), the expression of STAT3 showed a decreasing trend. In addition, the regulation of EAHDW on STAT3 translation and phosphorylation in Jurkat cells were studied with western blot (Figure 4D).

Finally, we performed an immunohistochemical study of STAT3 in mice kidneys. The result in Figure 4E shows. The STAT3 was hybridized with a specific antibody, which was in brown color. Moreover, the density of STAT3 was quantitatively analyzed and present in Figure 4F. The result showed that EAHDW could significantly inhibit the expression of STAT3 in the kidney of MRL/lpr mice. Interestingly, the low dose EAHDW application showed better activity than that of high dose EAHDW. However, no statistical difference between the two groups was observed. These results indicated that EAHDW could reduce the pathological changes of kidney tissue in MRL/lpr mice by regulating the STAT3.

### 3.6. Molecular docking mode predicted STAT3 regulator

Some publications reported the blocking capability of herbal ingredients on STAT3. We used the STAT3 docking model to screen the ingredients in EAHDW. The compounds, berberine (-6.9), asperuloside (-6.8), deacetyl asperulosidic acid methyl ester (-6.4), 10-deacetyl asperulosidic acid (-6.3), and geniposide (-6.1), had relative high docking affinity scores  $< -6$ . In detail, TRP-501 of STAT3 can form hydrogen bonds with berberine; LEU-1525, THR-1526, TYR-1539, and SER-1540 with Asperuloside; ARG-246, LEU-263, GLU-239, and LEU-260 deacetyl asperulosidic acid methyl ester; THR-1138, ASP-1242, VAL-1136, GYS-1259 with 10-deacetylasperulosidic acid; THR-1526, ASN-1538, SER-1540, and TYR-1539 with geniposide (Figure 5). Hence, these components may be key STAT3 regulators in EAHDW.

## 4. Discussion

SLE is characterized by secretion and production of multiple inflammatory cytokines, immune complexes, and autoantibodies, which can precipitate in different organs to induce dysfunction (Ohl and Tenbrock, 2011). *Hedyotis diffusa* Willd is one herbal consist of Jieduquyuziyin prescription, which showed beneficial effects in clinical therapy for SLE treatment (Ji et al., 2019). The clinical evidence indicated that HDW has a therapeutic effect in inflammatory and tumor diseases (Yan et al., 2017; Chen et al., 2016). However, less of the biological and pharmacological mechanism was known. The result of our previous studies (still under review) showed that the ethyl acetate extract of HDW (EAHDW) might be one of the active fractions. In this study, EAHDW was obtained by reflux and successive extraction. The extraction ratio was  $2.7 \pm 1\%$ . Geniposide, a major iridoid glycoside in nature, is one of the chemical constituents in HDW (Shan et al., 2017; Ma et al., 2016). Our result indicated that it was EAHDW with a concentration of 8.21% (g/g). Many types of research identified the presence of

geniposide in HDW or HDW extract. However, few quantitative studies were published. The molecular and debris mass of some ingredients in EAHDW were evaluated with UPLC-Q/TOF-MS. Nineteen of them were identified by comparing with the mass database of TCMs. The function of these nineteen ingredients was predicted with a network pharmacological study. The results indicated that regulation of T cell proliferation through STAT3 signaling pathway in SLE patients might be the major capability of EAHDW. Finally, we demonstrated this prediction with MRL/lpr mice *in vivo*, as well as a dual-fluorescence reporter assay and Jurkat cell assays *in vitro*. *In vivo* study, EAHDW showed attenuative activity on expression of inflammatory cytokines, synthesis of autoantibodies, pathological changes and STAT3 expression in the glomerulus. And *in vitro* studies, EAHDW showed regulative capability on STAT3 expression and phosphorylation. Simultaneously, EAHDW had regulative activity on T cell proliferation by affecting the cell cycle. In the molecular docking analysis, we predicted the blocking activity of five ingredients in EAHDW on the DNA binding site of STAT3.

The pharmacological and phytochemical researches of HDW have been carried for a period of time. The previous studies proved that EAHDW has the regulative activity of the cell cycle and proliferation. The ethyl acetate fraction in a mixture of HDW and *Scutellaria barbata* showed anti-inflammatory and anti-tumor effects by regulating miR155, PD-L1, and JNK signaling pathways (Xu et al., 2018; Yang et al., 2020). Our previous work (on publishing) also demonstrated that EAHDW is the main active fraction in HDW. However, fewer of the chemical composition studies were published. Therefore, we initially used UPLC-Q/TOF-MS to present the phytochemical character of EAHDW. UPLC-Q/TOF-MS is widely used to identify the known chemicals by comparing them with the mass of the standards and debris ions. The results identified a total of 19 components in the positive ion mode. Wang Y et al. identified 80 common components of *Hedyotis diffusa* with UPLC-Q/TOF-MS analysis (Wang et al., 2018). However, only four of them, asperuloside, geniposide, syringaldehyde and quinic acid, were identified in our study. It may be depended on the different extraction protocols and TCM database. Firstly, EAHDW is one of medal polar fractions in the total extract of HDW. Otherwise, some molecular may hydrolyze during the extraction process. Based on this result, a network pharmacological analysis was engaged to predict the potential targets of EAHDW on SLE treatment.

Network pharmacology is an analytical method to study the relationship between drugs, compounds, diseases, and targets. It is currently widely used to clarify the pharmacological mechanism of Chinese medicine (Xiong et al., 2021). Liu X et al. found that cell cycle and apoptosis were highly involved in the regulation of HDW on gastric cancer, of which the targets regulated by HDW are significantly related to signal pathways of cell cycle and apoptosis (Liu et al., 2018). In addition, Song Y et al. analyzed the regulative targets of HDW on prostate cancer. The results showed that multiple cancer-related pathways, such as angiogenesis, cell differentiation, apoptosis, and invasion, etc. were involved, and IL-6 and STAT3 signaling pathways were highlighted (Song et al., 2019). Similar to these previous studies, the network pharmacology analysis of EAHDW on SLE was closely related to the cell cycle, as well as T cell receptors, and TNF.

Abnormal activation of T cells plays an important role in the process of SLE. In 2014, Anselm Mak reviewed the pathological character of T cells in SLE, in which summarized some clinical cases of manipulating T cells in SLE (Mak and Kow, 2014). In 2019, a study demonstrated that cryptotanshinone treatment improved the pathological damage of SLE by inhibiting T cell proliferation (Du et al., 2019). The previous studies announced the T cells promoting activities of EAHDW on normal Balb/c and Balb/c leukemia mice, as well as HDW on C57BL/6 mice (Lin et al., 2011; Kuo et al., 2015). This seems utterly inconsistent with ours. It may be dependent on the mice model. *In vivo*, we did not quantify the T cells content directly, but the concentration of autoantibodies and inflammatory cytokines such as TNF, IL-6, IFN, IL-12, MCP-1, and IL-10 in serum were significantly attenuated by EAHDW treatment (Table 2, Table 3). TNF, IL-6, and IFN are secreted by T cells (Mehta et al., 2018; Li et al.,

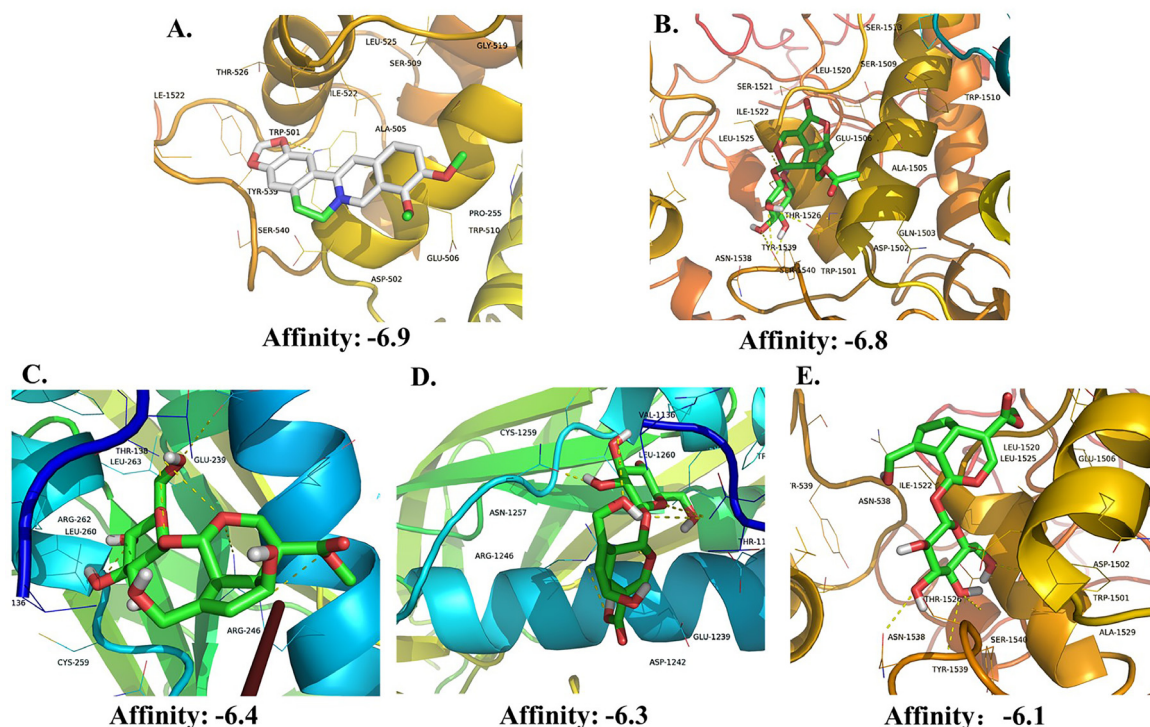


**Figure 5.** Molecular docking model of five ingredients binding to STAT3. (A.) Berberine, (B.) Asperuloside, (C.) Deacetyl asperulosidic acid methyl ester, (D.) 10-Deacetyl asperulosidic acid, (E.) Geniposide shown as 3D diagrams. The yellow dashed line indicates the hydrogen bond.

2018; Crouse et al., 2015). And IL-12 could induce T cell proliferation (Kieper et al., 2001). *In vitro*, the Jurkat cell cycle was influenced by EAHDW (Figure 4B), which showed inhibitory activity on cell proliferation (Figure 4A).

The abnormal activation of T cells is often accompanied by the enhancement of the JAK/STAT3 signaling pathway (Tsokos et al., 2003; Crispin et al., 2010). In our preliminary experiments, we found that Jurkat cells are more sensitive to EAHDW treatment than 293T cells. We hypothesized that it may be due to different cell lines that have different trends. In this research, we observed that the high concentration EAHDW (>25  $\mu\text{g}/\text{mL}$ ) treatment could stimulate the LIF-induced over-expression of STAT3 in 293T cells (Figure 4C) and phosphorylation of STAT3 in Jurkat cells (Figure 4D). LIF, a most pleiotropic member of the IL-6 cytokine family, is regarded as a potential marker of SLE activity, could significantly stimulate the expression of STAT3 (Nicola and Babon, 2015; Heinrich et al., 2003). LIF first binds to its signaling receptor LIF-R, and recruits another signaling receptor, glycoprotein 130 (GP130), to form a heterodimer that mediates downstream signal transduction. Upon dimerization, the signaling receptors recruit and phosphorylate JAKs, which, in turn, phosphorylate STAT3 (Viillard et al., 1999; Onishi and Zandstra, 2015). The enhancement of STAT3 in T cells not only promotes the secretion of inflammatory cytokines but also stimulates the abnormal proliferation of T cells. Previous studies have demonstrated that T cells in SLE patients showed a high content of phosphorylated STAT3, which improved differentiation and migration of T cells and promoted the B cell responses (Linterman et al., 2009; Harada et al., 2007). In the immunohistochemical study, we also found abnormal expression of STAT3 in MRL/lrp mice kidneys (Figure 4E, 4F). As we proposed that EAHDW treatment could attenuate this overdose expression in model mice. Otherwise, the results of cytological studies testified the STAT3 transcriptional and phosphorylated activities of EAHDW. In addition, 5 constituents in EAHDW showed potential docking activity on the reactive center of STAT3. Although, this is not the pioneer study to investigate the regulatory activity of EAHDW on STAT3. However, this study indicated that EAHDW can influence the prolifer-

ation of T cells via the STAT3 pathway, thereby improving SLE. This work clarified a little mechanism of HDW in clinical treatment of SLE. Future studies should exploit more SLE attenuation activities, as well as the pharmacological and phytochemical mechanism of EAHDW, more in detail.

## 5. Conclusion

*Hedyotis diffusa* Willd, one of the herbs consist of Jieduquyuziyin prescription, had glomerulus protection against autoantibody and inflammatory cytokines production activities on SLE model mice. And the ethyl acetate fraction of HDW could affect T cell proliferation by regulating STAT3 expression and phosphorylation. Otherwise, five ingredients contained berberine, asperuloside, deacetyl asperulosidic acid methyl ester, 10-deacetyl asperulosidic acid, and geniposide in EAHDW might inhibit the STAT3 activity by blocking the DNA binding site.

## Ethical Approval

The animal care and use committee of Zhejiang Chinese Medical University had approved the study protocol with certificate number 12322.

## Data Availability

All the raw data of this research are available per E-mail db@zcmu.edu.cn.

## Funding

This work was financially supported by the National Basic Research Program of China (973 Program, Grant No.2014CB543000) and Natural Science Foundation of China (81673857).

## Declaration of Competing Interest

All authors of this manuscript declared that no conflict of interest exists.

## CRediT authorship contribution statement

Yahui Lai: Methodology, Investigation, Data Curation, Writing - Original Draft. Jinjun Ji: Methodology. Ying Li: Software, Visualization. Jingqun Liu: Visualization. Xinhui Lan: Data Curation. Weihong Ge: Supervision. Li Xu: Conceptualization, Funding acquisition. Yongsheng Fan: Supervision, Project administration. Bin Ding: Methodology, Supervision, Validation, Writing - Review & Editing.

## Acknowledgements

We thank the college of Zhejiang Chinese Medical University laboratory animal research center for their great help on animal handle and experiments.

## ORCID

Bin Ding, <https://orcid.org/0000-0002-4009-5820>.

## Supplementary materials

All the raw data of this research are available per E-mail [db@zcmu.edu.cn](mailto:db@zcmu.edu.cn).

## References

- Caielli, S., Veiga, D.T., Balasubramanian, P., Athale, S., Domic, B., Murat, E., Banchereau, R., Xu, Z., Chandra, M., Chung, C.H., Walters, L., Baisch, J., Wright, T., Punaro, M., Nassi, L., Stewart, K., Fuller, J., Ucar, D., Ueno, H., Zhou, J., Pascual, V., 2019. A CD4+ T cell population expanded in lupus blood provides B cell help through interleukin-10 and succinate. *Nat. Med.* 25 (1), 75–81. doi:10.1038/s41591-018-0254-9.
- Chen, A., Xiong, P., Li, F., Zhang, L., Fu, J., Pan, Z., Li, W., Song, Z., Zhan, L., Zhu, F., Jin, S., 2005. Effect of YangYin Qingre Decoction on Expression of Adhesion Molecules and Lupus Index in the Patients with Systemic Lupus Erythematosus. *Chin. Med. J.* 06, 433–435. doi:10.13288/j.11-2166/r.2005.06.024.
- Chen, Y., Lin, Y., Li, Y., Li, C., 2016. Total flavonoids of *Hedyotis diffusa* Willd inhibit inflammatory responses in LPS-activated macrophages via suppression of the NF- $\kappa$ B and MAPK signaling pathways. *Exp. Therapeutic Med.* 11 (3), 1116–1122. doi:10.3892/etm.2015.2963.
- Crispin, J.C., Kyttaris, V.C., Terhorst, C., Tsokos, G.C., 2010. T cells as therapeutic targets in SLE. *Nature reviews. Rheumatology* 6 (6), 317–325. doi:10.1038/nrrheum.2010.60.
- Crouse, J., Kalinke, U., Oxenius, A., 2015. Regulation of antiviral T cell responses by type I interferons. *Nature reviews. Immunology* 15 (4), 231–242. doi:10.1038/nri3806.
- Durcan, L., O'Dwyer, T., Petri, M., 2019. Management strategies and future directions for systemic lupus erythematosus in adults. *Lancet (London, England)* 393 (10188), 2332–2343. doi:10.1016/s0140-6736(19)30237-5.
- Durant, L., Watford, W.T., Ramos, H.L., Laurence, A., Vahedi, G., Wei, L., Takahashi, H., Sun, H.W., Kanno, Y., Powrie, F., O'Shea, J.J., 2010. Diverse targets of the transcription factor STAT3 contribute to T cell pathogenicity and homeostasis. *Immunity* 32 (5), 605–615. doi:10.1016/j.immuni.2010.05.003.
- Du, Y., Du, L., He, Z., Zhou, J., Wen, C., Zhang, Y., 2019. Cryptotanshinone ameliorates the pathogenesis of systemic lupus erythematosus by blocking T cell proliferation. *Int. Immunopharmacol.* 74, 105677. doi:10.1016/j.intimp.2019.105677.
- Edwards, L.J., Mizui, M., Kyttaris, V., 2015. Signal transducer and activator of transcription (STAT) 3 inhibition delays the onset of lupus nephritis in MRL/lpr mice. *Clin. Immunol.* 158 (2), 221–230. doi:10.1016/j.clim.2015.04.004. Doi:10.1016/j.clim.2015.04.004.
- Harada, T., Kyttaris, V., Li, Y., Juang, Y.T., Wang, Y., Tsokos, G.C., 2007. Increased expression of STAT3 in SLE T cells contributes to enhanced chemokine-mediated cell migration. *Autoimmunity* 40 (1), 1–8. doi:10.1080/08916930601095148.
- Heinrich, P.C., Behrmann, I., Haan, S., Hermanns, H.M., Müller-Newen, G., Schaper, F., 2003. Principles of interleukin (IL)-6-type cytokine signalling and its regulation. *Biochem. J.* 374 (Pt 1), 1–20. doi:10.1042/BJ20030407. doi.org/.
- Ji, L., Hou, X., Deng, X., Fan, X., Zhuang, A., Zhang, X., Li, R., 2019. Jieduquyuziyin Prescription-Treated Rat Serum Suppresses Activation of Peritoneal Macrophages in MRL/lpr Lupus Mice by Inhibiting IRAK1 Signaling Pathway. Evidence-based complementary and alternative medicine: eCAM 2019, 2357217. doi:10.1155/2019/2357217. doi:10.1155/2019/2357217.
- Katsuyama, T., Li, H., Comte, D., Tsokos, G.C., Moulton, V.R., 2019. Splicing factor SRSF1 controls T cell hyperactivity and systemic autoimmunity. *J. Clin. Invest.* 129 (12), 5411–5423. doi:10.1172/JCI127949. doi:10.1172/JCI127949.
- Kieper, W.C., Prlic, M., Schmidt, C.S., Mescher, M.F., Jameson, S.C., 2001. IL-12 enhances CD8 T cell homeostatic expansion. *J. Immunol.* 166 (9), 5515–5521. doi:10.4049/jimmunol.166.9.5515.
- Kuo, Y.J., Lin, J.P., Hsiao, Y.T., Chou, G.L., Tsai, Y.H., Chiang, S.Y., Lin, J.G., Chung, J.G., 2015. Ethanol Extract of *Hedyotis diffusa* Willd Affects Immune Responses in Normal Balb/c Mice In Vivo. *In Vivo* 29 (4), 453–460 PMID: 26130790.
- La Paglia, G., Leone, M.C., Lepri, G., Vagelli, R., Valentini, E., Alunno, A., Tani, C., 2017. One year in review 2017: systemic lupus erythematosus. *Clin. Exp. Rheumatol.* 35 (4), 551–561 PMID: 28721860.
- Li, B., Jones, L.L., Geiger, T.L., 2018. IL-6 Promotes T Cell Proliferation and Expansion under Inflammatory Conditions in Association with Low-Level ROR $\gamma$ t Expression. *J. Immunol.* 201 (10), 2934–2946. doi:10.4049/jimmunol.1800016.
- Lin, C.C., Kuo, C.L., Lee, M.H., Hsu, S.C., Huang, A.C., Tang, N.Y., Lin, J.P., Yang, J.S., Lu, C.C., Chiang, J.H., Chueh, F.S., Chung, J.G., 2011. Extract of *Hedyotis diffusa* Willd influences murine leukemia WEHI-3 cells in vivo as well as promoting T- and B-cell proliferation in leukemic mice. *In vivo (Athens, Greece)*, 25 (4), 633–640 PMID: 21709007.
- Lin, J., Li, Q., Chen, H., Lin, H., Lai, Z., Peng, J., 2015. *Hedyotis diffusa* Willd. extract suppresses proliferation and induces apoptosis via IL-6-inducible STAT3 pathway inactivation in human colorectal cancer cells. *Oncol. Lett.* 9 (4), 1962–1970. doi:10.3892/ol.2015.2956.
- Lin, J.X., Leonard, W.J., 2018. The Common Cytokine Receptor  $\gamma$  Chain Family of Cytokines. *Cold Spring Harb. Perspect. Biol.* 10 (9), a028449. doi:10.1101/cshperspect.a028449.
- Lin, M., Lin, J., Wei, L., Xu, W., Hong, Z., Cai, Q., Peng, J., Zhu, D., 2012. *Hedyotis diffusa* Willd extract inhibits HT-29 cell proliferation via cell cycle arrest. *Exp. Therapeutic Med.* 4 (2), 307–310. doi:10.3892/etm.2012.599.
- Linterman, M.A., Rigby, R.J., Wong, R.K., Yu, D., Brink, R., Cannons, J.L., Schwartzberg, P.L., Cook, M.C., Walters, G.D., Vinuesa, C.G., 2009. Follicular helper T cells are required for systemic autoimmunity. *J. Exp. Med.* 206 (3), 561–576. doi:10.1084/jem.20081886.
- Liu, X., Wu, J., Zhang, D., Wang, K., Duan, X., Meng, Z., Zhang, X., 2018. Network Pharmacology-Based Approach to Investigate the Mechanisms of *Hedyotis diffusa* Willd. in the Treatment of Gastric Cancer. Evidence-based complementary and alternative medicine: eCAM 2018, 7802639. doi:10.1155/2018/7802639.
- Ma, H., Li, F.L., Wang, F., Guo, Q., Cao, G.S., Yang, P.M., 2016. *Zhong yao cai. J. Chin. Med. Mater.* 39 (1), 98–102 PMID: 30080008.
- Mak, A., Kow, N.Y., 2014. The pathology of T cells in systemic lupus erythematosus. *J. Immunol. Res.* 2014, 419029. doi:10.1155/2014/419029.
- Mehta, A.K., Gracias, D.T., Croft, M., 2018. TNF activity and T cells. *Cytokine* 101, 14–18. doi:10.1016/j.cyto.2016.08.003.
- Nicola, N.A., Babon, J.J., 2015. Leukemia inhibitory factor (LIF). *Cytokine Growth Factor Rev.* 26 (5), 533–544. doi:10.1016/j.cytogfr.2015.07.001. doi.org/.
- Ohl, K., Tenbrock, K., 2011. Inflammatory cytokines in systemic lupus erythematosus. *Journal of biomedicine & biotechnology* 2011, 432595. doi:10.1155/2011/432595.
- Onishi, K., Zandstra, P.W., 2015. LIF signaling in stem cells and development. *Development* 142 (13), 2230–2236. doi:10.1242/dev.117598. doi.org/.
- Shan, M., Yu, S., Yan, H., Guo, S., Xiao, W., Wang, Z., Zhang, L., Ding, A., Wu, Q., Li, S., 2017. A Review on the Phytochemistry, Pharmacology, Pharmacokinetics and Toxicology of Geniposide, a Natural Product. *Molecules* 22 (10), 1689. doi:10.3390/molecules22101689. doi.org/.
- Song, Y., Wang, H., Pan, Y., Liu, T., 2019. Investigating the Multi-Target Pharmacological Mechanism of *Hedyotis diffusa* Willd Acting on Prostate Cancer: A Network Pharmacology Approach. *Biomolecules* 9 (10), 591. doi:10.3390/biom9100591.
- Trott, O., Olson, A.J., 2010. AutoDock Vina: improving the speed and accuracy of docking with a new scoring function, efficient optimization, and multithreading. *J. Comput. Chem.* 31 (2), 455–461. doi:10.1002/jcc.21334.
- Tsokos, G.C., Nambiar, M.P., Tenbrock, K., Juang, Y.T., 2003. Rewiring the T-cell: signaling defects and novel prospects for the treatment of SLE. *Trends Immunol.* 24 (5), 259–263. doi:10.1016/s1471-4906(03)00100-5.
- Viallard, J.F., Taupin, J.L., Miossec, V., Pellegrin, J.L., Moreau, B.L., 1999. Analysis of interleukin-6, interleukin-10 and leukemia inhibitory factor (LIF) production by peripheral blood cells from patients with systemic lupus erythematosus identifies LIF as a potential marker of disease activity. *Eur. Cytokine Netw.* 10 (1), 17–24 PMID: 10210768.
- Wang, C., Zhou, X., Wang, Y., Wei, D., Deng, C., Xu, X., Xin, P., Sun, S., 2017. The Antitumor Constituents from *Hedyotis Diffusa* Willd. *Molecules* 22 (12), 2101. doi:10.3390/molecules22122101.
- Wang, Y., Wang, C., Lin, H., Liu, Y., Li, Y., Zhao, Y., Li, P., Liu, J., 2018. Discovery of the Potential Biomarkers for Discrimination between *Hedyotis diffusa* and *Hedyotis corymbosa* by UPLC-QTOF/MS Metabolome Analysis. *Molecules* 23 (7), 1525. doi:10.3390/molecules23071525.
- Xiong, Z., Zheng, C., Chang, Y., Liu, K., Shu, L., Zhang, C., 2021. Exploring the Pharmacological Mechanism of Duhuo Jisheng Decoction in Treating Osteoporosis Based on Network Pharmacology. Evidence-based complementary and alternative medicine: eCAM 2021, 5510290. doi:10.1155/2021/5510290.
- Xu, Y., Chen, X.X., Jiang, Y.X., Zhang, D.D., 2018. Ethyl Acetate Fraction from *Hedyotis diffusa* plus *Scutellaria barbata* Exerts Anti-Inflammatory Effects by Regulating miR-155 Expression and JNK Signaling Pathway. Evidence-based complementary and alternative medicine: eCAM 2018, 3593408. doi:10.1155/2018/3593408.
- Yang, L., Lin, S., Xu, L., Lin, J., Zhao, C., Huang, X., 2019. Novel activators and small-molecule inhibitors of STAT3 in cancer. *Cytokine Growth Factor Rev.* 49, 10–22. doi:10.1016/j.cytogfr.2019.10.005.
- Yang, Y., Fang, T., Cao, Y.L., Lv, Y.X., Chang, Q.Q., Zhang, D.D., 2020. Ethyl Acetate Fraction from *Hedyotis diffusa* plus *Scutellaria barbata* Exerts Anti-Breast Cancer Effect via

- miR-200c-PDE7B/PD-L1-AKT/MAPK Axis. Evidence-based complementary and alternative medicine: eCAM 2020, 3587095. doi:[10.1155/2020/3587095](https://doi.org/10.1155/2020/3587095).
- Yan, Z., Feng, J., Peng, J., Lai, Z., Zhang, L., Jin, Y., Yang, H., Chen, W., Lin, J., 2017. Chloroform extract of *Hedyotis diffusa* Willd inhibits viability of human colorectal cancer cells via suppression of AKT and ERK signaling pathways. *Oncol. Lett.* 14 (6), 7923–7930. doi:[10.3892/ol.2017.7245](https://doi.org/10.3892/ol.2017.7245).
- Yoshida, N., He, F., Kytтары, V.C., 2019. T cell-specific STAT3 deficiency abrogates lupus nephritis. *Lupus* 28 (12), 1468–1472. doi:[10.1177/0961203319877242](https://doi.org/10.1177/0961203319877242).
- Zhang, L., Wei, W., 2020. Anti-inflammatory and immunoregulatory effects of paeoniflorin and total glucosides of paeony. *Pharmacol. Ther.* 207, 107452. doi:[10.1016/j.pharmthera.2019.107452](https://doi.org/10.1016/j.pharmthera.2019.107452).